Active Colloidal Suspensions Exhibit Polar Order under Gravity

Mihaela Enculescu and Holger Stark

Institut für Theoretische Physik, Technische Universität Berlin, Hardenbergstrasse 36, 10623 Berlin, Germany

(Received 13 February 2011; published 28 July 2011)

Recently, the steady sedimentation profile of a dilute suspension of chemically powered colloids was studied experimentally [J. Palacci *et al.*, Phys. Rev. Lett. **105**, 088304 (2010)]. It was found that the sedimentation length increases quadratically with the swimming speed of the active Brownian particles. Here we investigate theoretically the sedimentation of self-propelled particles undergoing translational and rotational diffusion. We find that the measured increase of the sedimentation length is coupled to a partial alignment of the suspension with the mean swimming direction oriented against the gravitational field. We suggest realistic parameter values to observe this polar order. Furthermore, we find that the dynamics of the active suspension can be derived from a generalized free energy functional.

DOI: 10.1103/PhysRevLett.107.058301 PACS numbers: 82.70.Dd, 47.57.ef, 47.63.Gd

Swimming cells use a variety of mechanisms to propel themselves in a viscous environment [1]. A common property of swimming cells is that they actively move along a swimming direction defined by their cell body, in contrast to passive cells suspended in water that move only by diffusion. This internally generated, active motion leads to interesting collective phenomena that have been a subject of great interest in the last years [2–6]. We show here that, even in very dilute suspensions, self-propelled Brownian particles develop polar order in an external field such as gravitation.

Several studies report the emergence of long-range orientational order in systems of active particles. In most cases, the orientational anisotropy is due to the specific particle interaction considered: Approaches based on the Vicsek model [2,7] assume that self-propelled particles align locally with neighbors. Inelastic collisions have been found to be at the origin of nematic alignment of rodlike particles [8]. Biologically motivated pursuit and escape interactions lead to the formation of coherently moving clusters and vortex structures [9]. Instabilities generated by hydrodynamic interactions can also result in long-range alignment of active particle suspensions [3,10,11] or the formation of swarms in harmonic traps [6]. Highly concentrated actin filaments propelled by molecular motors on motility assays can self-organize to form coherently moving structures [12]. In contrast to these examples, we report on a system of noninteracting active particles that shows polar order. Anisotropy is generated here by the interplay between self-propulsion and an external force that does not affect directly the swimming direction.

Artificial self-motile colloidal particles have been designed recently using different techniques that allow control of the propulsion velocity as well as particle interactions [13]. One example is the study of sedimentation of active particles under gravity. It has been shown experimentally [14] and also predicted theoretically for run-and-tumble particles [5,15] that the sedimentation length of dilute active particle suspensions increases quadratically with their active velocity. We show here that this increase in sedimentation length goes hand in hand with the formation of polar order in the active particle suspension and also explains the colloid accumulation at the bottom surface observed in experiments [14]. Furthermore, we predict that with increasing particle radius the orientational order becomes more pronounced and should be directly observable in experiments.

Since the volume fraction of colloids in [14] was very small (0.05%), we neglect in the following any particle interactions and develop the theory for a gas of active Brownian particles. We start from the Langevin equations of motion and derive a Smoluchowski equation for the particle distribution in the overdamped limit. We finally reformulate it as a density functional theory.

We assume that each active particle swims with a constant speed v_0 in a particular direction given by the unit vector $\mathbf{p}$ and associated to the particle. This swimming velocity is added to the velocity, a passive particle would have due to external forces and interactions with the solvent. We describe each active spherical particle by its position $\mathbf{r}$, the direction of swimming $\mathbf{p}$, total velocity $\mathbf{v}$, and angular velocity $\boldsymbol{\omega}$. Considering the forces and torques experienced by a sedimenting particle in a viscous fluid, the Langevin equations of an active particle read

$$\dot{\mathbf{r}} = \mathbf{v}, \qquad \dot{\mathbf{v}} = -\frac{\gamma}{m}(\mathbf{v} - v_0\mathbf{p}) + v_0\boldsymbol{\omega}\times\mathbf{p} + \mathbf{g} + \boldsymbol{\zeta},$$
$$\dot{\mathbf{p}} = \boldsymbol{\omega}\times\mathbf{p}, \quad \dot{\boldsymbol{\omega}} = -\frac{\gamma_r}{I}\boldsymbol{\omega} + \boldsymbol{\eta}. \tag{1}$$

Here, γ and γ_r are the respective translational and rotational friction coefficients, m and I are the buoyant mass and the moment of inertia of the particles, respectively, and $\mathbf{g} = -g\mathbf{e}_z$ is the gravity field. A change of the particle orientation due to the interaction with the fluid results in the pseudoacceleration $v_0\boldsymbol{\omega}\times\mathbf{p}$. Without noise, the

swimming direction would be constant and the velocity of the particle would relax to $\mathbf{v} = v_0\mathbf{p} + m\mathbf{g}/\gamma$. With noise, the velocity changes due to random forces and torques. We assume the solvent is a thermal bath at temperature T so that the spheres experience additional stochastic translational and rotational accelerations $\boldsymbol{\zeta}$ and $\boldsymbol{\eta}$, the second moments of which fulfill the fluctuation-dissipation theorem: $\langle\boldsymbol{\zeta}(t)\boldsymbol{\zeta}(t')\rangle = (2\gamma k_BT/m^2)\delta(t-t')\mathbb{I}$, $\langle\boldsymbol{\eta}(t)\boldsymbol{\eta}(t')\rangle = (2\gamma_r k_BT/I^2)\delta(t-t')\mathbb{I}$.

Following the standard method [16], a Fokker-Planck equation for the one-particle distribution function $f(\mathbf{r}, \mathbf{p}, \mathbf{v}, \boldsymbol{\omega}, t)$ can be derived from the Langevin equations (1). The relaxation time m/γ of the particle velocity $\mathbf{v}$ can be estimated from [14] to be about 10 ns. The change of the position variable occurs about 10^8 times slower: $R/v_0 \sim 0.1$–1 s. On this time scale, the velocity distribution is relaxed to a Gaussian. A similar argument holds for the rotational velocities. This motivates a local-equilibrium Maxwell-Boltzmann approximation $f(\mathbf{r}, \mathbf{p}, \mathbf{v}, \boldsymbol{\omega}, t) \sim \rho(\mathbf{r}, \mathbf{p}, t)\exp\{-\beta m[(\mathbf{v} - \bar{\mathbf{v}}(\mathbf{r}, \mathbf{p}, t)]^2/2 - \beta I[\boldsymbol{\omega} - \bar{\boldsymbol{\omega}}(\mathbf{r}, \mathbf{p}, \mathbf{t})]^2/2\}$ [17] that leads to equations for the reduced distribution function $\rho(\mathbf{r}, \mathbf{p}, t)$, mean particle velocity $\bar{\mathbf{v}}$, and mean angular velocity $\bar{\boldsymbol{\omega}}$ at $(\mathbf{r}, \mathbf{p}, t)$:

$$\rho_t + \nabla\cdot(\rho\bar{\mathbf{v}}) + \mathcal{R}\cdot(\rho\bar{\boldsymbol{\omega}}) = 0,$$
$$\rho\frac{D(\bar{\mathbf{v}} - v_0\mathbf{p})}{Dt} + \frac{\gamma}{m}\rho(\bar{\mathbf{v}} - v_0\mathbf{p}) = -\frac{k_BT}{m}\nabla\rho + \mathbf{g}\rho, \qquad (2)$$
$$\rho\frac{D\bar{\boldsymbol{\omega}}}{Dt} + \frac{\gamma_r}{I}\rho\bar{\boldsymbol{\omega}} = -\frac{k_BT}{I}\mathcal{R}\rho.$$

Here, ∇ refers to the position coordinate $\mathbf{r}$, $\mathcal{R}$ denotes the rotation operator $\mathbf{p}\times\nabla_{\mathbf{p}}$, and $D/Dt = \partial_t + \bar{\mathbf{v}}\cdot\nabla + \bar{\boldsymbol{\omega}}\cdot\mathcal{R}$ is the material derivative. In the limit of vanishing Reynolds number, $D(\bar{\mathbf{v}} - v_0\mathbf{p})/Dt$ and $D\bar{\boldsymbol{\omega}}/Dt$ in Eqs. (2) are negligible with respect to the damping terms so that

$$\bar{\mathbf{v}} = v_0\mathbf{p} + \frac{m\mathbf{g}}{\gamma} - \frac{k_BT}{\gamma}\nabla\ln\rho, \quad \bar{\boldsymbol{\omega}} = -\frac{k_BT}{\gamma_r}\mathcal{R}\ln\rho. \qquad (3)$$

The reduced particle distribution function then obeys a Smoluchowski equation

$$\rho_t + \nabla\cdot J^t + \mathcal{R}\cdot J^r = 0, \qquad (4)$$

with the translational and rotational fluxes $J^t = -D\nabla\rho + (v_0\mathbf{p} + m\mathbf{g}/\gamma)\rho$ and $J^r = -D_r\mathcal{R}\rho$. Here, $D = k_BT/\gamma$ and $D_r = k_BT/\gamma_r$ are the constants of translational and rotational diffusion, respectively. For spheres of radius R, one has $D_r = 3D/4R^2$. Note that Eq. (4) can be derived also directly from the overdamped limit of Eqs. (1).

In Eq. (4), space and time can be rescaled according to $\mathbf{r}' = \mathbf{r}/R$ and $t' = tD/R^2$. With $\mathbf{g} = -g\mathbf{e}_z$ and in terms of the new coordinates, the Smoluchowski equation reads

$$\rho_{t'} = \nabla'^2\rho + \frac{3}{4}\mathcal{R}^2\rho - (\mathrm{Pe}\mathbf{p} - \alpha\mathbf{e}_z)\cdot\nabla'\rho, \qquad (5)$$

and contains now only two dimensionless parameters: the active Peclet number $\mathrm{Pe} = v_0R/D$ and the gravitational Peclet number $\alpha = mgR/k_BT$. They compare either active swimming or gravitation-induced drift motion to thermal diffusion.

For passive particles, the steady state of Eq. (5) is given by the well-known barometric formula $\rho \sim \exp(-\alpha z')$. Experiments in [14] confirm the exponential decay for the *total* density of active particles with a velocity-dependent sedimentation length. However, it can be easily shown that Eq. (5) has no isotropic steady state: For such a state, the contribution of the rotational diffusion $\mathcal{R}^2\rho$ would vanish, but the balance of the diffusion and drift terms would depend explicitly on the swimming direction: $\rho \sim \exp[-(\alpha - \mathrm{Pe}p_z)z']$. This observation and the experimentally measured total density profile suggest the following ansatz for the steady state:

$$\rho(\mathbf{r}, \mathbf{p}) \sim e^{(-\alpha z'/\xi)}e^{[\mathrm{Pe}U_1(\cos\theta) + \mathrm{Pe}^2U_2(\cos\theta) + \cdots]}, \qquad (6)$$

where we use the axial symmetry of the problem around the z axis and introduce the angle θ with $\cos\theta = \mathbf{p}\cdot\mathbf{e}_z$. The coefficient $\xi = \delta_{\mathrm{eff}}/\delta_0$ describes the ratio between the effective sedimentation length of active particles and the sedimentation length $\delta_0 = R/\alpha$ of passive particles. Classical perturbation theory in Pe leads to $\xi(\mathrm{Pe}, \alpha) = 1 + \frac{2}{9}\mathrm{Pe}^2 - \mathcal{O}(\mathrm{Pe}^4, \alpha^1)$, which recovers in second order the result found in [14] and fits experimental data very well up to $\mathrm{Pe} = 5$. However, we also find nonvanishing higher-order terms in Pe with coefficients depending on the gravitational Peclet number α. The first coefficient functions in Eq. (6) are given by $U_1 = 2\alpha\cos\theta/3$, $U_2 = -2\alpha^2\cos^2\theta/27$.

From Eq. (5), a Smoluchowski equation for the total density $\Omega(\mathbf{r}, \mathbf{t}) = \oint\rho(\mathbf{r}, \mathbf{p})d^2p$ follows by integrating over all orientations:

$$\Omega_{t'} = \Omega_{z'z'} - \mathrm{Pe}(\langle\cos\theta\rangle\Omega)_{z'} + \alpha\Omega_{z'}. \qquad (7)$$

Thereby, $\langle\cos\theta\rangle = \oint p_z\rho(\mathbf{r}, \mathbf{p}, \mathbf{t})d^2p/\Omega$ characterizes the mean orientation of the particles along the vertical. Equation (7) states that besides the diffusive and gravitational particle currents, there is also a drift current initiated by a polar ordering of the active particles. Hence, in a steady density profile active particles partially align against gravity field. Integrating Eq. (6) over all directions gives $\Omega \sim e^{-\alpha z'/\xi}$, and then Eq. (7) leads to

$$\mathrm{Pe}\langle\cos\theta\rangle = \alpha + \frac{\Omega_z'}{\Omega} = \frac{\alpha(\xi - 1)}{\xi} > 0 \quad \text{for } \xi > 1. \qquad (8)$$

The mean orientation given in Eq. (8) depends nonmonotonically on the Peclet number Pe. Within the second-order approximation of ξ in Pe, it has a maximum $\alpha/3\sqrt{2}$ at $\mathrm{Pe} = 3/\sqrt{2}$.

Equation (7) is only the first one of a hierarchy of equations for the moments $\langle\cos^n\theta\rangle$. The dynamics of the mean orientation $\langle\cos\theta\rangle$ can be derived by multiplying Eq. (5) with $\cos\theta$ and integrating over all orientations. The resulting equation depends on the unknown $\langle\cos^2\theta\rangle$,

etc. For small perturbations around the steady state, the leading terms in Pe lead to $\langle\cos\theta\rangle = -2/9\,\mathrm{Pe}\Omega_{z'}/\Omega$ and Eq. (7) reduces to the Smoluchowski equation derived in [14]: $\Omega_{t'} - [(1 + 2/9\,\mathrm{Pe}^2)\Omega_{z'} + \alpha\Omega]_{z'} = 0$. However, for big Peclet numbers or far from steady state, no effective dynamics for the total density can be derived, since the above hierarchy cannot be closed.

Figure 1 compares numeric solutions of Eq. (5) with the second-order approximation of the reduced effective sedimentation length $\xi = \delta_{\mathrm{eff}}/\delta_0 = 1 + 2/9\,\mathrm{Pe}^2$ and the corresponding expression for $\langle\cos\theta\rangle$ in Eq. (8). Graphs (a),(b) show both quantities for fixed α and variable Pe. Both $\alpha = 0.1$ and the range of Pe correspond to values used in the experiments of [14]. As in Ref. [14], the second-order correction fits the sedimentation length very well (b). However, the polar order in Fig. 1(a) deviates from the second-order approximation in the convection dominated regime for $\mathrm{Pe} > 2$. Moreover, for the experimental parameter $\alpha \sim 0.1$ it is smaller than 2.5%. We, therefore, compare in Fig. 1(c) the predicted linear dependence of $\langle\cos\theta\rangle$ on α to the numerical solution. Since $\alpha \sim R^4$, taking colloids with a radius of 1 μm instead of 0.5 μm (used in [14]) would increase the mean orientation of particles from 2.5% to 20%. So the anisotropy in the particle orientation could be directly observed. Note that α is also increased when tuning g in a centrifuge. By contrast, δ_{eff} increases only slowly with α [Fig. 1(d)], and this dependence results from a higher-order approximation of ξ. Both sedimentation length δ_{eff} and mean alignment $\langle\cos\theta\rangle$ saturate when α increases further and a perfectly ordered state occurs for $\alpha \to \infty$. However, for $\alpha > 1$ or $\delta_0 < R$, passive particles accumulate at the bottom. So active particles need a sufficiently large swimming velocity v_0 to create a continuous density profile.

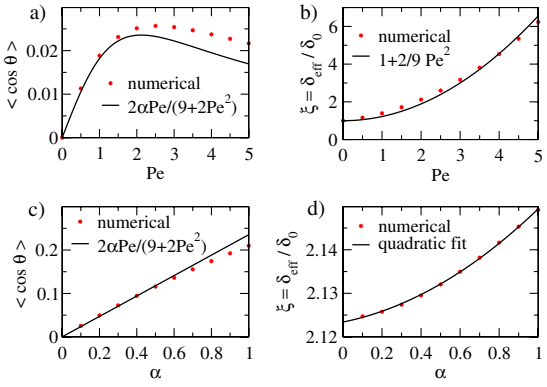

FIG. 1 (color online). Dependence of polar order and reduced sedimentation length on $\mathrm{Pe} = v_0 R/D$ and $\alpha = R/\delta_0$: (a), (b) $\langle\cos\theta\rangle$ and ξ as a function of Pe for $\alpha = 0.1$; (c), (d) $\langle\cos\theta\rangle$ and ξ as a function of α for $\mathrm{Pe} = 2$. Numerical data are computed from the steady solution of Eq. (5) by $\delta_{\mathrm{eff}}/\delta_0 = -\alpha\Omega/\Omega_z$ and the definitions of Ω and $\langle\cos\theta\rangle$ (see text).

At bounding walls, the balance of diffusive, active, and gravitational currents has to vanish for each orientation, so the boundary condition reads: $0 = \rho_{z'} + (\alpha - \mathrm{Pe}\cos\theta)\rho$. Close to the walls, our numerical solution deviates from the exponential decay in the bulk given by Eq. (6) [see Fig. 2(a)]. Because of the boundary, particles swimming against the wall ($\theta = \pi$) accumulate and there is a depletion of particles swimming away from the wall ($\theta = 0$) [see Fig. 2(a)]. Figure 2(b) shows the angular distribution of the particles at different altitudes z^*. Far from the wall, the particle distribution has a maximum for particles swimming up (blue curve) whereas close to the bottom wall, most particles are swimming down (black curve). This leads to a strong polar order at the wall. The total density profile $\Omega(z)$ [see Fig. 2(c)] reflects this strong ordering with a sharp decay close to the wall at large Pe before it enters the predicted and measured exponential decay. In Fig. 2(d), we discard the first microns. Then the renormalized profiles show very good agreement with the experimental data in Fig. 3 of [14]. There, data from the first 4 μm are also not shown. The authors only mention a strong accumulation of particles at the bottom surface and attribute it to colloid adsorption. However, our theory shows that this accumulation is solely due to the particle's active motion. We noticeably observe this effect also at the upper wall for $\mathrm{Pe} \geq 4$ (corresponding profiles not shown in [14]).

The steady state of the active Brownian gas differs from the passive case also by the fact that the mean translational and rotational velocities $\bar{\mathbf{v}}$ and $\bar{\boldsymbol{\omega}}$ of the local Maxwell-Boltzmann approximation do not vanish. From Eqs. (3) and (6) it follows

$$\bar{\mathbf{v}}^{\mathrm{SS}} = v_0\mathbf{p} + \frac{m\mathbf{g}}{\gamma}\frac{\xi - 1}{\xi},$$

$$\bar{\boldsymbol{\omega}}^{\mathrm{SS}} = \left(\frac{\beta m v_0}{2} + v_0^2 \cdots\right)\mathbf{p} \times \mathbf{g}.$$

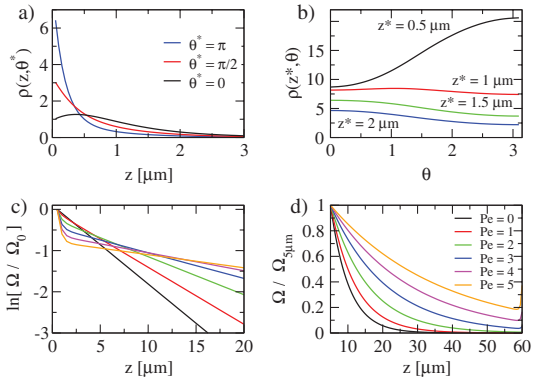

FIG. 2 (color). (a) Altitude dependence of the particle distribution $\rho(z, \theta^*)$ for different orientations θ^*. (b) Angular dependence of $\rho(z^*, \theta)$ at different heights z^*. (c) Logarithmic plot of the normalized total density $\Omega(z)$ [see (d) for legend]. (d) Rescaled density profiles after discarding the first micrometers. Parameter values: $\alpha = 1$, $\mathrm{Pe} = 2$ (a),(b) and $\alpha = 0.1$ (c),(d).

Except for these mean translational and rotational velocities, the active suspension sediments like a passive suspension in an effective potential $U_{\text{eff}}(\mathbf{r}, \mathbf{p})$, which we identify as in [18] by writing Eq. (6) as $\rho(\mathbf{r}, \mathbf{p}) \sim \exp[-\beta U_{\text{eff}}(\mathbf{r}, \mathbf{p})]$. With this potential we define an effective free energy $F = F^{\text{id}} + \int \oint U_{\text{eff}}(\mathbf{r}, \mathbf{p}) \rho(\mathbf{r}, \mathbf{p}) d^3 r d^2 p$, where F^{id} denotes the free energy of an ideal gas. Remarkably, the evolution of the active suspension described by Eq. (4) then takes the form

$$\rho_t = \nabla \cdot \left[\rho \left(\frac{1}{\gamma} \nabla \frac{\delta F}{\delta \rho} - \bar{\mathbf{v}}^{\text{SS}} \right) \right] + \mathcal{R} \cdot \left[\rho \left(\frac{1}{\gamma_r} \mathcal{R} \frac{\delta F}{\delta \rho} - \bar{\boldsymbol{\omega}}^{\text{SS}} \right) \right]. \tag{9}$$

Equation (9) can also be derived for interacting active particles if the system exhibits a steady state. Then a uniquely defined effective free energy F exists together with mean velocities $\bar{\mathbf{v}}^{\text{SS}}$ and $\bar{\boldsymbol{\omega}}^{\text{SS}}$ [19]. We interpret Eq. (9) as a dynamic density functional theory (DDFT) for a system of active particles [20]. A previous attempt at a DDFT for active particles uses the free energy functional of passive particles, and neglects therefore any active contributions to the particle correlations [21]. However, this approximation cannot reproduce all aspects shown by Brownian dynamics simulations. Here, we propose to derive the dynamics from the effective free energy of the active steady state instead of the free energy corresponding to passive particles. The generic conditions for the existence of active steady states are still unknown. It was shown recently that hydrodynamic interactions between sedimenting active particles might still allow for a steady state [6].

In conclusion, we have derived a Smoluchowski equation for a gas of noninteracting active Brownian particles under gravity. We find that sedimentation is accompanied by polar order of the active particles and enhanced orientational ordering at surfaces. Our discussion in terms of the active (Pe) and gravitational (α) Peclet numbers shows that the polar order can easily be increased to measurable values. Our Smoluchowski equation can immediately be formulated for any external potential and it would be interesting to study the gas of active Brownian particles in different situations.

We have constructed an effective free energy functional for a gas of noninteracting active Brownian particles in a gravitational field. Under the condition that a steady state of an active particle suspension exists, we have formulated a dynamic density functional theory. This theory can be generalized to interacting particles and therefore provides an appealing approach for exploring the dynamics of dense active suspensions. The challenging task is to identify the effective free energy for given particle interactions.

We thank R. Golestanian for helpful discussions and the Deutsche Forschungsgemeinschaft for financial support through the research training group GRK1558.

[1] D. Bray, *Cell Movements. From Molecules to Motility* (Garland Publishing, New York, 2001); H. A. Stone and A. D. T. Samuel, Phys. Rev. Lett. **77**, 4102 (1996); E. Lauga and T. Powers, Rep. Prog. Phys. **72**, 096601 (2009).
[2] T. Vicsek *et al.*, Phys. Rev. Lett. **75**, 1226 (1995).
[3] R. A. Simha and S. Ramaswamy, Phys. Rev. Lett. **89**, 058101 (2002).
[4] L. Schimansky-Geier, M. Mieth, H. Rose, and H. Malchow, Phys. Lett. A **207**, 140 (1995); U. Erdmann, W. Ebeling, and A. S. Mikhailov, Phys. Rev. E **71**, 051904 (2005); E. Bertin, M. Droz, and G. Gregoire, *ibid.* **74**, 022101 (2006); D. Saintillan and M. J. Shelley, Phys. Rev. Lett. **99**, 058102 (2007); B. Lindner and E. Nicola, Eur. Phys. J. Special Topics **157**, 43 (2008); D. Loi, S. Mossa, and L. F. Cugliandolo, Phys. Rev. E **77**, 051111 (2008); R. Golestanian, Phys. Rev. Lett. **102**, 188305 (2009).
[5] J. Tailleur and M. Cates, Europhys. Lett. **86**, 60 002 (2009).
[6] R. W. Nash, R. Adhikari, J. Tailleur, and M. E. Cates, Phys. Rev. Lett. **104**, 258101 (2010).
[7] F. Peruani, A. Deutsch, and M. Bär, Eur. Phys. J. Special Topics **157**, 111 (2008); H. Chate, F. Ginelli, and R. Montagne, Phys. Rev. Lett. **96**, 180602 (2006).
[8] A. Kudrolli, G. Lumay, D. Volfson, and L. S. Tsimring, Phys. Rev. Lett. **100**, 058001 (2008); F. Ginelli, F. Peruani, M. Bär, and H. Chate, *ibid.* **104**, 184502 (2010).
[9] P. Romanczuk, I. D. Couzin, and L. Schimansky-Geier, Phys. Rev. Lett. **102**, 010602 (2009).
[10] D. Saintillan and M. J. Shelley, Phys. Rev. Lett. **100**, 178103 (2008).
[11] T. Ishikawa and T. J. Pedley, Phys. Rev. Lett. **100**, 088103 (2008); A. Bashkaran and M. Marchetti, Proc. Natl. Acad. Sci. U.S.A. **106**, 15 567 (2009).
[12] V. Schaller *et al.*, Nature (London) **467**, 73 (2010).
[13] W. Paxton *et al.*, J. Am. Chem. Soc. **126**, 13 424 (2004); R. Dreyfus *et al.*, Nature (London) **437**, 862 (2005); J. Howse *et al.*, Phys. Rev. Lett. **99**, 048102 (2007); S. Ebbens *et al.*, Phys. Rev. E **82**, 015304 (2010).
[14] J. Palacci, C. Cottin-Bizonne, C. Ybert, and L. Bocquet, Phys. Rev. Lett. **105**, 088304 (2010).
[15] J. Tailleur and M. E. Cates, Phys. Rev. Lett. **100**, 218103 (2008).
[16] H. Risken, *The Fokker-Planck Equation. Methods of Solution and Applications* (Springer, New York, 1996).
[17] A. Archer, J. Chem. Phys. **130**, 014509 (2009).
[18] J. Prost, J. F. Joanny, and J. M. R. Parrondo, Phys. Rev. Lett. **103**, 090601 (2009).
[19] M. Enculescu and H. Stark (unpublished).
[20] U. Marconi, J. Chem. Phys. **110**, 8032 (1999); A. Archer and R. Evans, *ibid.* **121**, 4246 (2004); M. Rex, H. H. Wensink, and H. Löwen, Phys. Rev. E **76**, 021403 (2007).
[21] H. H. Wensink and H. Löwen, Phys. Rev. E **78**, 031409 (2008).